JOURNAL OF APPLIED ELECTROCHEMISTRY 23 (1993) 641–645

Mechanistic study of the hydrogen evolution reaction on Ni–Zn and Ni–S cathodes*

M. J. DE GIZ, M. FERREIRA, G. TREMILIOSI-FILHO, E. R. GONZALEZ

Departamento de Físico-Química, IFQSC/USP, C.P. 369, São Carlos, SP 13560, Brazil

Received 7 July 1992; revised 15 October 1992

Electrodeposited Ni–Zn and Ni–S on a mild steel substrate have shown very good performance as cathode materials for the HER in alkaline media. The materials were studied previously with surface techniques and evaluated through current–potential curves and long term operation. This paper describes a detailed mechanistic study of the HER on Ni–Zn and Ni–S carried out with impedance techniques. In both cases the reaction proceeds through a Volmer–Heyrovsky mechanism. As predicted by kinetic theory, the temperature study shows that the energy of activation of the rate determining step is the same as the energy of activation of the overall reaction.

1. Introduction

In recent years much attention has been given to nickel alloys as suitable electrode materials for the hydrogen evolution reaction (HER) in alkaline media as improved alternatives to traditional materials like mild steel, used in unipolar electrolysers or electrodeposited nickel employed in bipolar electrolysers [1–4]. Most studies were carried out by recording current–potential curves and then analysing the corresponding Tafel parameters and the dependence of the current and overpotential with pH. The parameters obtained were then compared with those predicted by classical electrochemical theories. From a mechanistic point of view, this approach is very limited but led to the conclusion that the improved performance of the material can be attributed to a true electrocatalytic effect, to a substantial increase in effective electrochemical area or both. Unless a detailed mechanistic study of the reaction is carried out it is not always obvious which is the most important effect on a given material. Thus, it is important to use more powerful methods to study the HER and gather fundamental data that may lead to the design of new materials with improved performance. As shown by Conway *et al.*, potential decay [5] and impedance spectroscopy [6–8] proved to be powerful tools to determine the kinetics and mechanism of the hydrogen evolution reaction and have helped substantially to the present knowledge of this process.

Several electrodeposited nickel-based alloys have been developed in this laboratory that present a much better performance than either mild steel or electrodeposited nickel, the traditional materials used as cathodes in unipolar and bipolar electrolysers, respectively [9]. With the idea of obtaining a high area material electrodeposits of Ni–Zn were produced on mild steel. After leaching part of the zinc with KOH solution a high area material was obtained (roughness factor ~ 1130). The performance of this material was studied through current-potential curves and continuous operation and the surface characterized with SEM, X-ray and cyclic voltammetric techniques [10]. Chen and Lasia [11] recently reported a mechanistic study of the HER on Ni–Zn. Their study considered different alloy compositions but did not include temperature effects. On the other hand, electrodeposits of Ni–S were also prepared and studied with the same techniques because of the low cost of preparation and the good long term performance [9, 12]. This material gives sufficiently low overpotentials although its roughness factor is relatively low (~ 130) [9]. Because of the differences in composition and surface structure and morphology a detailed mechanistic study on these two materials with a powerful technique may provide substantial information for the design of better electrocatalysts for the HER. Thus, it was decided to carry out a mechanistic study of the HER in alkaline media, including the effect of temperature, on Ni–Zn and Ni–S cathodes using impedance techniques.

2. Experimental details

Details of the preparation of the materials by electrodeposition and their characterization were already given in the literature for Ni–Zn [10] and Ni–S [9]. Electrochemical experiments were done in a three compartment glass cell. The counter electrode was a platinum foil and the system $Hg/HgO/HO^-$ was used as reference, separated from the main compartment with a Luggin capillary. EDX analysis of the cathode surface even after long term electrolysis showed no sign of platinum contamination from the counter electrode [10]. Solutions were prepared with KOH (BDH, Aristar) and water purified in a Milli-Pore system. Impedance measurements were carried out with a Solartron 1250 frequency response analyser and a

* This paper is dedicated to Professor Brian E. Conway on the occasion of his 65th birthday, and in recognition of his outstanding contribution to electrochemistry.

0021-891X

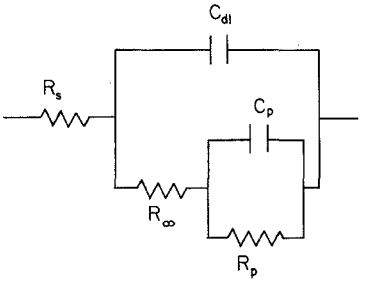

Scheme 1. Equivalent circuit for the HER.

Solartron 1286 potentiostat coupled to a HP 9000 (series 300) computer for data aquisition and processing. Measurements were performed at cathodic overpotentials ranging from -0.05 to -0.45 V, selected from the linear portion of the Tafel plot. The amplitude of the sinusoidal perturbation was 10 mV. Ten frequency points per decade were used in the range 10^{-2}–10^4 Hz. Steady state current–potential data were obtained galvanostatically with a PAR 273 potentiostat with ohmic drop compensation. All experiments were done at 0, 25, 40, 60 and 80° C.

3. Results and discussion

In this work it is assumed that the hydrogen evolution reaction in alkaline media proceeds according to the usual mechanism:

$$M + H_2O + e^- \underset{k_{-1}}{\overset{k_1}{\rightleftarrows}} MH + HO^- \quad (1)$$

$$MH + H_2O + e^- \xrightarrow{k_2} M + H_2 + HO^- \quad (2)$$

or

$$MH + MH \xrightarrow{k_3} 2M + H_2 \quad (3)$$

where Steps 2 and 3 can be alternative or simultaneous. Since the reaction involves an adsorbed intermediate the process can be represented from the point

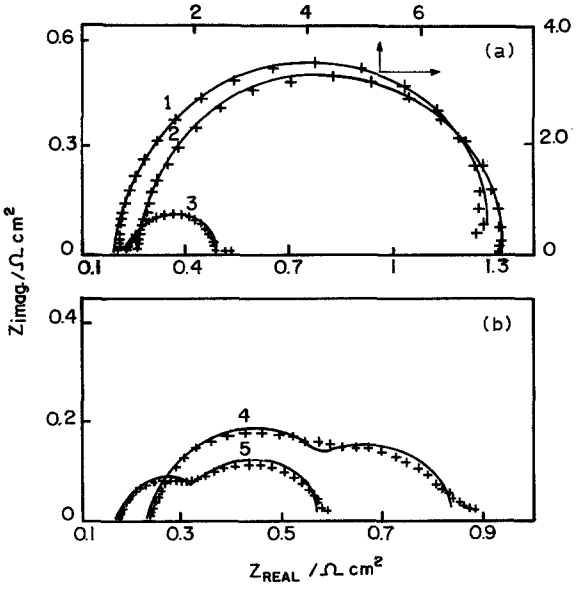

Fig. 1. Impedance plots for the HER on Ni–Zn (1) 0, (2) 25, (3) 40, (4) 60 and (5) 80° C. (a) $\eta = -90$ mV; (b) $\eta = -60$ mV. (+) Experimental points; (——) simulation results.

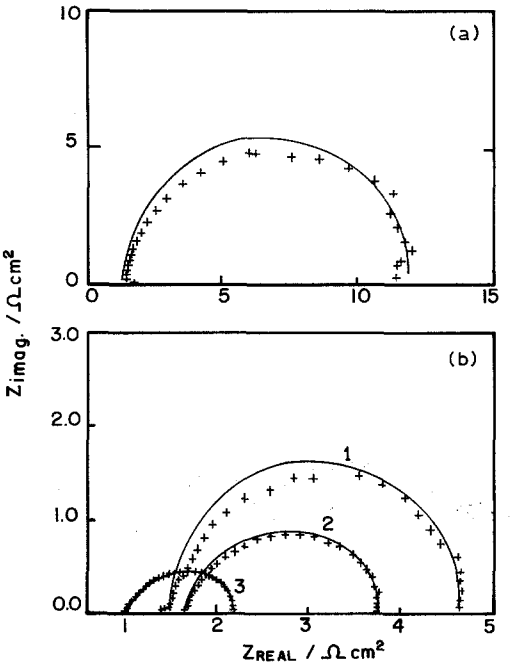

Fig. 2. Impedance plots for the HER on Ni–S. (a) 0° C, $E = -1.18$ V; (b) (1) 25, (2) 40 and (3) 60° C, $E = -1.22$ V. (+) Experimental points; (——) simulation results.

of view of its electrochemical response by the equivalent circuit proposed by Armstrong *et al.* [13, 14] (Scheme 1). In this scheme, R_s is the solution resistance, R_∞ is the charge transfer resistance and the parallel combination R_p/C_p simulates the behaviour of the adsorbed intermediate. Here, it is assumed that diffusion is much faster than charge transfer, so it has no effect on the measured parameters. Obviously, the circuit parameters R_∞, R_p and C_p are related to the mechanism of the reaction and their values are dependent on the values of k_1, k_{-1}, k_2 and k_3, as shown by Harrington and Conway [6]. Thus, impedance plots can be generated from the values of the rate constants. The actual calculations were done through simulation procedures on the same computer as used in the experimental measurements.

Figure 1 shows the experimental and the simulated plots in the complex impedance plane for the HER on Ni–Zn at five different temperatures and close values of the potential. From the equivalent circuit shown in Scheme 1 it would be expected that a complex impedance plot would generate two semicircles. This is indeed observed at 60 and 80° C, while at lower temperatures only one semicircle is present. This is because in this case the impedance is dominated by the parallel combination C_p/R_p to such an extent that only one semicircle is detected. The corresponding results for Ni–S are presented in Fig. 2, and it must be noted that, contrary to the case of Ni–Zn, there is only one semicircle at all temperatures indicating a still greater influence of C_p/R_p. The simulated plots were obtained by giving suitable values to the rate constants, the transfer coefficients and the maximum coverage with hydrogen in the overpotential region. In all cases a good agreement between the experimental results and the simulated plots exists and from these the rate

Table 1. Values of the rate constants for the HER on Ni–Zn and Ni–S at different temperatures

Material	*T* /°C	k_1 /mol cm^{-2} s^{-1}	k_{-1} /mol cm^{-2} s^{-1}	k_2 /mol cm^{-2} s^{-1}	k_3 /mol cm^{-2} s^{-1}
Ni–Zn	0	0.20×10^{-6}	0.23×10^{-5}	0.06×10^{-7}	0.20×10^{-13}
	25	0.80×10^{-6}	0.81×10^{-5}	0.46×10^{-7}	0.68×10^{-13}
	40	1.40×10^{-6}	9.70×10^{-5}	1.50×10^{-7}	1.30×10^{-13}
	60	0.64×10^{-6}	5.40×10^{-5}	1.70×10^{-7}	2.80×10^{-13}
	80	1.20×10^{-6}	3.80×10^{-5}	3.40×10^{-7}	2.80×10^{-13}
Ni–S	0	1.00×10^{-8}	0.07×10^{-4}	0.09×10^{-9}	1.00×10^{-14}
	25	1.00×10^{-8}	0.03×10^{-4}	0.30×10^{-9}	1.00×10^{-14}
	40	1.00×10^{-8}	0.20×10^{-4}	1.56×10^{-9}	1.00×10^{-14}
	60	1.00×10^{-8}	3.70×10^{-4}	3.20×10^{-9}	1.00×10^{-14}

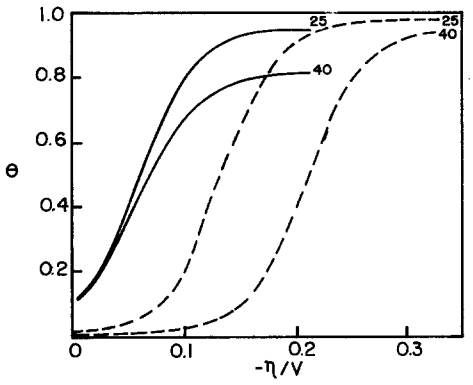

Fig. 3. Hydrogen coverage as a function of the overpotential for Ni–Zn (full line) and Ni–S (broken line) at two temperatures indicated on the curves.

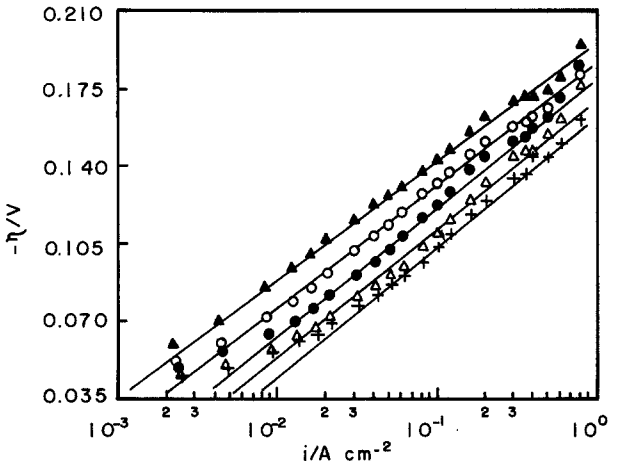

Fig. 4. Tafel plots at different temperatures for Ni–Zn. (▲) 25, (○) 40, (●) 50, (△) 60 and (+) 70° C.

constants presented in Table 1 were obtained. The values of the rate constants lead to the conclusion that on both materials the HER follows a Volmer–Heyrovsky mechanism with the Heyrovsky step (Reaction 2) being rds. This should be taken as a working assumption because, as pointed out by Lasia and Rami [15], it is impossible to decide from the experimental results whether the Volmer or the Heyrovsky step is rate determining.

The values in Table 1 also explain unambiguously the better performance of Ni–Zn for the HER. This material gives values of k_1 and k_2 which are two orders of magnitude larger than those for Ni–S at all temperatures. Taking into account that the roughness factor of Ni–Zn is only an order of magnitude larger than that of Ni–S it must be concluded that Ni–Zn has not only a larger effective area but also a better intrinsic electrocatalytic activity than Ni–S. Because the catalytic activity is usually related to the characteristics of adsorption of intermediates it is of interest to compare the behaviour of the two materials with respect to this aspect. Figure 3 shows the coverage with adsorbed hydrogen as a function of the overpotential for Ni–Zn and Ni–S at 25 and 40° C. It is interesting to note that the rising part of the curves for Ni–Zn starts at low overpotentials and is almost independent of temperature, indicating a strong adsorption. For Ni–S similar coverages are obtained at significantly higher overpotentials. Furthermore, the influence of temperature is much more pronounced in the sense that at higher temperatures, higher overpotentials are required to obtain similar coverages, which indicates that the adsorption of the intermediate is weaker than in the case of Ni–Zn.

The HER on Ni–Zn cathodes with different compositions was also studied by Chen and Lasia [11] with impedance methods but only at 25° C. Their results show that, for a nickel content similar to that employed in this work (28% Ni before leaching), the values of k_1 are smaller than those presented here while those of k_2 are very similar. Also, for the same nickel content their

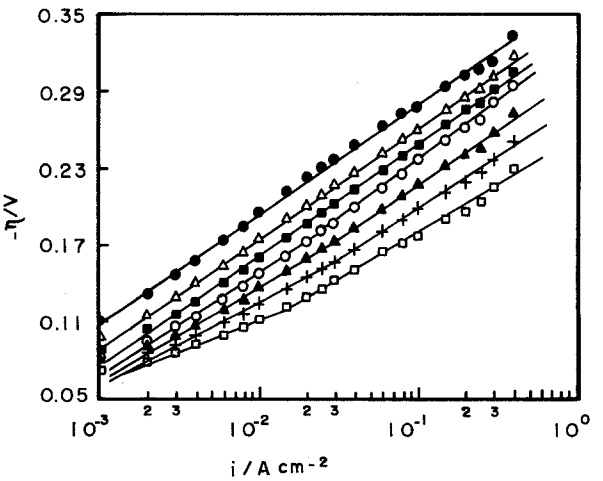

Fig. 5. Tafel plots at different temperatures for Ni–S. (●) 25, (△) 30, (■) 40, (○) 50, (▲) 60, (+) 70 and (□) 80° C.

Table 2. Electrochemical parameters obtained from the plots in Figs 4 and 5. b = Tafel slope, i_0 = exchange current density

T /°C	Ni–Zn		Ni–S			
	b /mV dec^{-1}	$i_0 \times 10^3$ /A cm^{-2}	b /mV dec^{-1}	$i_0 \times 10^4$ /A cm^{-2}	b* /mV dec^{-1}	$i_0^* \times 10^4$ /A cm^{-2}
25	55	0.234	85	0.513	–	–
30	–	–	85	0.847	–	–
40	57	0.499	86	1.290	–	–
50	60	0.918	78	1.200	95	3.340
60	63	1.660	68	0.910	86	2.990
70	60	1.820	58	0.666	82	3.750
80	–	–	47	0.393	73	3.810

* Values for the high current density region

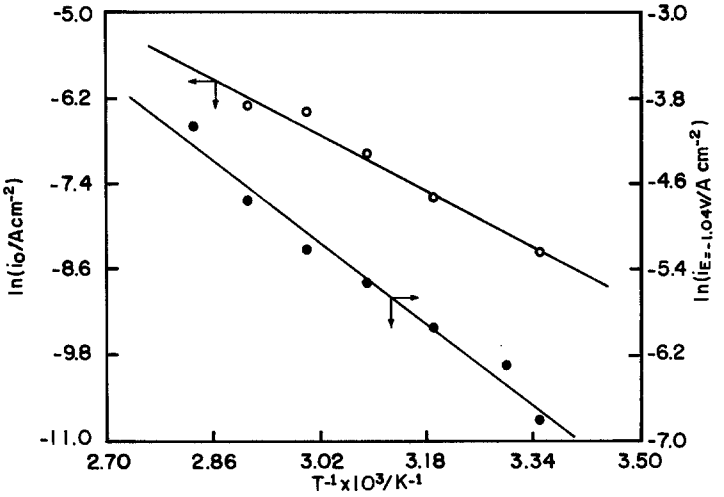

Fig. 6. Arrhenius plots for the HER (○) from the values of i_0 for Ni–Zn and (●) from the values of i at −1.04 V for Ni–S.

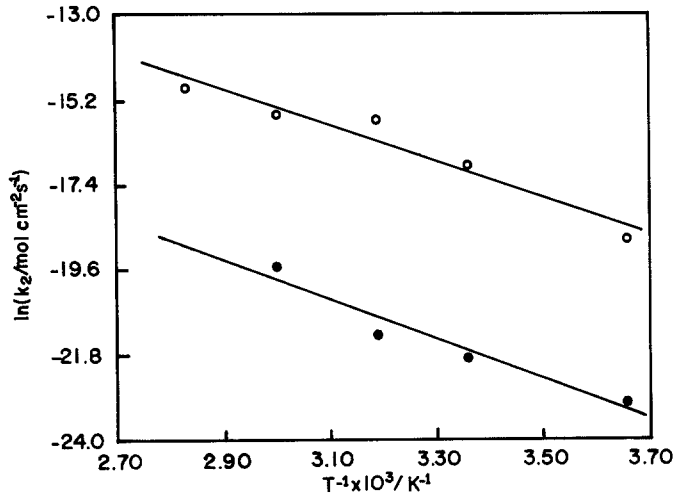

Fig. 7. Arrhenius plots from the values of k_2 for (○) Ni–Zn and (●) Ni–S.

roughness factor is ~1000 which is very near the value for the material used in this work (~1130). One possibility of explaining the values of k_1 is that, because of differences in the preparation and treatment, the behaviour of the material used in this work is more characteristic of an alloy, which presents an enhanced catalytic activity toward the Volmer reaction.

A very interesting aspect of the impedance study of the HER, not explored so far, is the fact that the values of the rate constants at different temperatures allow a determination of the energy of activation of the rate determining step. If the analysis is consistent this must be the same as the energy of activation of the overall reaction, which can be obtained from polarization curves. Figures 4 and 5 show experimental steady state current–potential data in the form of Tafel plots at different temperatures for Ni–Zn and Ni–S, respectively. The corresponding Tafel parameters are presented in Table 2. For Ni–Zn, the overall Arrhenius plot, presented in Fig. 6 was constructed using the

values of i_0. On the other hand, for Ni–S the extrapolated Tafel plots at low current densities cross each other, precluding the possibility of using the values of i_0 to construct an Arrhenius plot. This is apparent by examining the values of i_0 in Table 2. Anomalies of this type in the Tafel slopes have been discussed by Conway *et al.* [16, 17] and attributed to the particular ways in which the coverage with adsorbed hydrogen depends on overpotential. Therefore, the Arrhenius plot for Ni–S, included in Fig. 6, was constructed using the values of the current densities at -1.04 V. The values of the energy of activation from the plots in Fig. 6 were 41 and 39 kJ mol^{-1} for Ni–Zn and Ni–S, respectively.

Figure 7 shows the Arrhenius plots constructed with the values of k_2 in Table 2. From these, the values of the energy of activation were 39 and 42 kJ mol^{-1} for Ni–Zn and Ni–S, respectively. Within experimental error these values may be considered equal to those obtained from the Tafel plots. This fact, which is consistent with fundamental kinetic theory, supports the procedures used in this work to treat the impedance results.

Acknowledgements

Thanks are due to the Fundação de Amparo a Pesquisa do Estado de São Paulo (FAPESP) and the Conselho Nacional de Desenvolvimento Científico e Technológico (CNPq) for financial support.

References

[1] H. Wendt and G. Imarisio, *J. Appl. Electrochem.* **18** (1988) 1.
[2] J. Divisek, P. Malinowski, J. Mergeland and H. Schmitz, *Int. J. Hydogen Energy* **13** (1988) 141.
[3] I. Arul Raj and K. I. Vasu, *J. Appl. Electrochem.* **20** (1990) 32.
[4] Y. Choquette, L. Brossard and H. Ménard, *ibid.* **20** (1990) 855.
[5] B. E. Conway and L. Bai, *Int. J. Hydrogen Energy* **11** (1986) 533.
[6] D. A. Harrington and B. E. Conway, *Electrochim. Acta* **32** (1987) 1703.
[7] L. Bai, D. A. Harrington and B. E. Conway, *ibid.* **32** (1987) 1713.
[8] L. Bai and B. E. Conway, *J. Electrochem. Soc.* **138** (1991) 2897.
[9] M. J. de Giz, J. C. P. Silva, M. Ferreira, S. A. S. Machado, E. A. Ticianelli, L. A. Avaca and E. R. Gonzalez *Int. J. Hydrogen Energy* **17** (1992) 725.
[10] M. J. de Giz, S. A. S. Machado, L. A. Avaca and E. R. Gonzalez, *J. Appl. Electrochem.* **22** (1992) 973.
[11] L. Chen and A. Lasia, *J. Electrochem. Soc.* **138** (1991) 3321.
[12] E. R. Gonzalez, L. A. Avaca, G. Tremiliosi-Filho, S. A. S. Machado and M. Ferreira, Proceedings of the IX World Hydrogen Energy Conference, Paris, France, July 1992.
[13] R. D. Armstrong and M. Henderson, *J. Electroanal. Chem.* **9** (1972) 81.
[14] R. D. Armstrong, R. E. Firman and H. R. Thirsk, *Faraday Disc. Chem. Soc. Lond.* **56** (1973) 244.
[15] A. Lasia and A. Rami, *J. Electroanal. Chem.* **294** (1990) 123.
[16] B. E. Conway, D. F. Tessier and D. P. Wilkinson, *J. Electroanal. Chem.* **199** (1986) 249.
[17] B. E. Conway, D. F. Tessier and D. P. Wilkinson, *J. Electrochem. Soc.* **136** (1989) 2436.